Finite Element Discretization of the Continuous Conductivity Equation for Squared Rectangular and Cubed Parallelepiped Networks

Aaron J. Shock

June 18, 2003

1 Introduction

This paper is primarily concerned with the inverse problem of recovering tile-wise constant conductivities from a perfectly sqaured rectangular mesh with potentials and currents defined at the nodal point corners of the mesh tiles. The complete formulation of this problem includes a finite element discretization of the continuous conductivity equation, as well as the construction and analysis of Kirchhoff and response matrices. In § 2, we describe the continous Dirichlet problem related to these tile conductivity networks and generate the corresponding finite element discretization. In § 3 we construct a sample (mxn)-tile conductivity network. Finally, in § 4 and 5, we discuss preliminary findings with respect to (mxn)-tile networks.

2 The Dirichlet Problem and Dirichlet-Neumann Map

Let us begin our discussion by formally constructing the Dirichlet problem and subsequent Dirichlet-to-Neumann map for our discretization of the continuous problem. Take a perfectly squared rectangular (n x m)-tile conductivity network T with $2(n+m)$ boundary nodes, and define strictly positive scalat tile conductivities $\{\gamma_1, \ldots, \gamma_{nm}\}$. Given some combination of boundary data from ϕ and/or ψ, determine a γ-harmonic function u such that u equals v on the interior of T and equals ϕ on the boundary of T. Specifically, we are looking for a function u such that

$$\vec{u} = \begin{bmatrix} \vec{\phi} \\ \vec{v} \end{bmatrix} \qquad\qquad div\,(\gamma \nabla u) = 0 \qquad \mathrm{int} T$$

The next goal will be to construct a Dirichlet-to-Neumann map from the function u such that when applied to the boundary potentials ϕ provides the boundary currents ψ, either entering or exiting the network. In matrix form, we are looking for a function Ku that generates a Dirichlet-to-Neumann map Λ such that the following properties hold.

$$K\vec{u} \quad = \quad \begin{bmatrix} \vec{\psi} \\ \vec{0} \end{bmatrix} \qquad \longmapsto \qquad \Lambda\vec{\phi} \quad = \quad \vec{\psi}$$

2.1 Minimization of the Energy Principle

First, take the vector u to represent all nodal potentials in our network, as was noted in the previous section. Then, consider the quadratic form of a function in u that represents power, analogous to $p = (1/r)v^2 = \gamma v^2$ as

$$Q(u,u) \quad = \quad \iint_T \gamma |\nabla u|^2 \, \mathrm{d}A$$

The goal here is to discretize the minimization of energy over the tile network with respect to piecewise constant conductivities and piecewise bilinear (PB) potential functions. So then, assign a separate scalar conductivity, denoted γ_k, and a PB potential function U_k defined over each tile. Specifically, for unit side-length tiles normally aligned with the planar coordinate axis as in Figure 1, the PB functions can be defined as follows

$$\begin{aligned} B_{0,0}(x,y) &= \begin{cases} (1-|x|)(1-|y|) & |x|,|y| \leq 1 \\ 0 & \text{otherwise} \end{cases} \\ B_{k,l}(x,y) &= B_{0,0}(k-x, l-y) \end{aligned}$$

where k and l represent integer coordinate offsets from the planar origin. This definition results in regions of local support for each PB potential function, such that $B_{k,l}$ takes on a value of 1 at its regional midpoint and diminishes to a value of 0 at the square boundary defined a unit distance away in either axial direction.

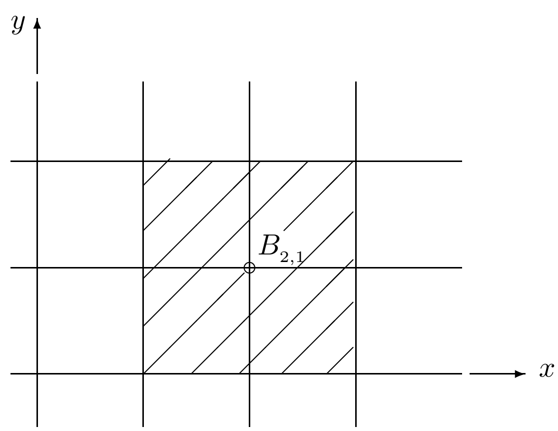

Figure 1: Region of Local Support for PB Potential Function

From here, we may also note that the PB potential function defined over a specific tile may be written as a linear combination of the PB functions defined at the four tile corners. So then, for some tile T_k, the potential function is given by

$$U_k = \sum_{i=1}^{4} \alpha_{ik} B_{ik}$$

where the constants α_{ik} represent the nodal potentials defined at the corners, and B_{ik} represent the PB functions with regions of local support centered at the corners of tile T_k. Subsequently, we can rewrite the original *power* function as follows, where $(M = mn)$ represents the number of tiles in our network.

$$\begin{aligned}
Q(U,U) &= \sum_{k=1}^{M} \gamma_{k} \iint_{T_k} \left|\nabla U_{k}\right|^2 \mathrm{d}A \\
&= \sum_{k=1}^{M} \gamma_{k} \iint_{T_k} \left\langle \sum_{i=1}^{4} \alpha_{ik} \nabla B_{ik}, \sum_{j=1}^{4} \alpha_{jk} \nabla B_{jk} \right\rangle \mathrm{d}A \\
&= \sum_{k=1}^{M} \sum_{i,j=1}^{4} \gamma_{k} \alpha_{ik} \alpha_{jk} \int_{T_k} \left\langle \nabla B_{ik}, \nabla B_{jk} \right\rangle \mathrm{d}A \qquad (1)
\end{aligned}$$

Then, noting that α_{ik} is chosen from the values of $\vec{u}$ and the integral over the inner product evaluates to a scalar, $Q(U,U)$ can be written in the symmetric, positive semi-definite bilinear form as

$$Q(U,U) = Q(u,u) = \sum_{r,s=1}^{(mn+m+n+1)} \kappa_{r,s} u_r u_s = u^T K u$$

From here, the approximation of the solution to the corresponding Dirichlet problem becomes that of finding the u that minimizes $Q(u,u)$ with respect to the space of piecewise bilinear functions. So to solve for any particular interior nodal potential, we differentiate Q with respect to the element in u corresponding to that interior node, set it equal to 0 and solve for the interior nodal potential in terms of the other potentials. So then for interior node i

$$\frac{\partial Q(u,u)}{\partial \vec{u}_i} = 0$$

Hence, the vector $\vec{u}$ is such that the above partial derivative is satisfied with respect to all of the interior nodal potentials in the tile network T. This leaves us with a system of $(nm - n - m + 1)$ algebraic equations to solve, as the null space parameterized in conductivities γ.

2.2 Kirchhoff and Response Matrices

By extracting the matrix K from the previous quadratic form, we can denote the entries $\kappa_{i,j}$ explicitly as

$$(\kappa_{i,j}) = \sum_{n} \iint_{T_k} \gamma_k \left\langle \nabla B_{ik}, \nabla B_{jk} \right\rangle \mathrm{d}A \qquad (2)$$

where n respresents the number of tiles where the PB functions about nodes i and j share local support, such that $n \in \{0, 1, 2\}$. It is then verifiable that the necessary properties for Kirchhoff matrices are indeed satisfied [1]. First, K is symmetric by construction such that $Ku = 0$ when

$u = constant \neq 0$. By square symmetry, K can be decomposed into a triangularized system such that $K = Z^T Z$. So then,

$$u^T K u \quad = \quad u^T Z^T Z u \quad = \quad |Zu|^2 \quad = 0$$

$$\Rightarrow \qquad Zu = 0 \qquad \Rightarrow \qquad Z^T Z u = 0 \qquad \Rightarrow \qquad Ku = 0$$

Specifically, by employing this argument with u equal to a vector of 1's, it is shown that the row and column sums of K are indeed zero.

To verify the the non-positive nature of off-diagonal entries in K, let us consider the three possible ways in which two PB potential functions can be related within a perfectly squared rectangular tile network. First, consider the case of two disjoint regions of local support as in the case between the PB functions defined about opposite corners of a multi-tile network. Then, indeed, the integral over the dot product of their gradients is zero because of their disjoint regions of support. Next, consider the possibility that two PB potential functions share two square regions of local support, as in Figure 2. Specifically, if we consider the PB potential functions with local support about nodes i and j as U_i and U_j, respectively, then they both contribute inner product terms over tiles 4 and 9 to the matrix K.

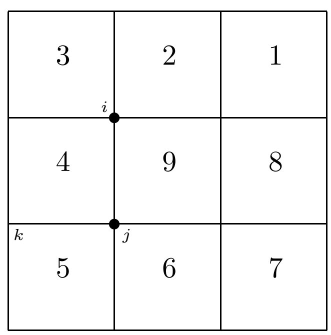

Figure 2: Negative $\kappa_{i,j}$ Entries $\sim$ Two-Tile Overlap

If we allow the normally oriented planar origin to run through node k, then the contributing term to $\kappa_{i,j}$ corresponding to tile 4 is given by

$$\begin{aligned} \kappa_{ij} &= \int_{T_4} \gamma_4 \left\langle \nabla (xy), \nabla (x - xy) \right\rangle \mathrm{d}A \\ &= \gamma_4 \int_0^1 \int_0^1 \left(y - y^2 - x^2 \right) \mathrm{d}x \, \mathrm{d}y \\ &= -\left(\frac{\gamma_4}{6} \right) \quad < \quad 0 \end{aligned}$$

Then, since the PB functions for both nodes i and j are symmetric across tiles 4 and 9, the total entry $\kappa_{i,j} = -\left(\frac{\gamma_4+\gamma_9}{6}\right)$. Therefore, in the case of two overlapping tiles of neighboring PB support, the off-diagonal entry of K is in fact negative. Next, consider a similar situation where two regions of PB support overlap on only one tile, as shown in Figure 3 with respect to the PB functions U_i and U_j that only have overlapping support on tile 9.

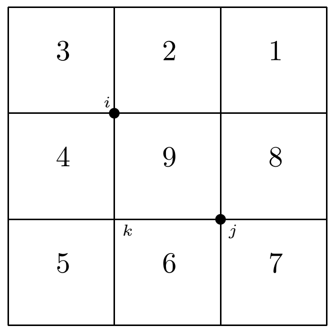

Figure 3: Negative $\kappa_{i,j}$ Entries $\sim$ One-Tile Overlap

If we allow the normally oriented planar origin to once again run through node k, then the contributing term to $\kappa_{i,j}$ corresponding to tile 4 is given by

$$\begin{aligned}
\kappa_{ij} &= \int_{T_9} \gamma_9 \left\langle \nabla\left(y - xy\right), \nabla\left(x - xy\right)\right\rangle \mathrm{d}A \\
&= \gamma_9 \int_0^1 \int_0^1 \left(-y + y^2 - x + x^2\right) \mathrm{d}x\,\mathrm{d}y \\
&= -\left(\frac{\gamma_9}{3}\right) \quad < \quad 0
\end{aligned}$$

So then, the matrix K is symmetric and positive semi-definite, and has row and column sums of zero. Furthermore, we have shown that all the off-diagonal entries κ_{ij} are non-positive. So then, K is truly a Kirchhoff matrix and subsequently represents some electrical network. Given this verification of K as a Kirchhoff matrix, we can then compute the response matrix Λ by means of the Schur complement [1].

$$K = \left(\begin{array}{c|c} A & B \\ \hline B^T & C \end{array}\right)$$

By this partitioning scheme, we derive the *response* matrix as the Schur complement of K in C such that

$$\Lambda = K/C = A - BC^{-1}B^T$$

The effect of the *response* matrix is that we may use Λ as a function upon the *boundary* potentials to compute the *boundary* currents as

$$\Lambda\phi \quad = \quad (K/C)\phi \quad = \quad (A - BC^{-1}B^T)\phi \quad = \quad \psi$$

3 $(m$x$n)$-Tile Network Construction

Consider the perfectly squared rectangular network of conductive tiles shown in Figure 4, where the *boundary* nodes are numbered beginning with 1 in the upper right corner, and prceeding in a counter-clockwise pattern through node $2(m+n)$ at the upper-most right node just below node 1. The *interior* nodes are thus numbered between $2(m+n)+1$ and $(mn+m+n+1)$, though the ordering is not significant at this point. Furthermore, note that the tile conductivities are numbered in a counter-clockwise manner, beginning in the top right corner and proceeding counter-clockwise through the outer-most ring of tiles. After this, the next-most outer ring of tiles will take on a similar numbering pattern, and so on until the highest numbered tile conductivities are found in the inner-most ring, row or column of the network.

4 Recovering Outer Ring Tile Conductivities

Next, consider the imposition of $2(m+n)$ *boundary* conditions as shown in Figure 5. From this configuration of *boundary* conditions, and through a continuation argument rooted in Kirchhoff's Law, the network in Figure 5 can be reduced to the greatly simplified row network shown in Figure 6. Before proceeding, however, let us note that there is a unique $(n-1)$-connection between *boundary* vertices with imposed currents and those *boundary* vertices with unknown potentials $\{c_1, \ldots, c_{n-1}\}$. This unique connection should be readily seen by beginning with the furthest left node of 0 current along the bottom row and noticing that the only path it can take to a node of unknown potential is to directly connect with the node labeld c_1. Proceeding successively to the right, it is shown that each *boundary* node with zero current can connect with only one choice of *boundary* node of unknown potential. So then, as shown by Morrow [1] (p.49), there exists a unique solution of the mixed Dirichlet-Neumann problem, which in this case translates into a unique optimal approximation to the vertex potentials defined by our PB discretization over the rectangular network. Hence, we can proceed under the assumption that the *boundary* potentials $\{c_1, \ldots, c_{n-1}\}$ are uniquely determinable by way of the current equations generable from our reduced network in Figure 6.

At this point, we can note a number of relationships among the various undetermined potentials c_i. First, the potential c_1 can be written as the

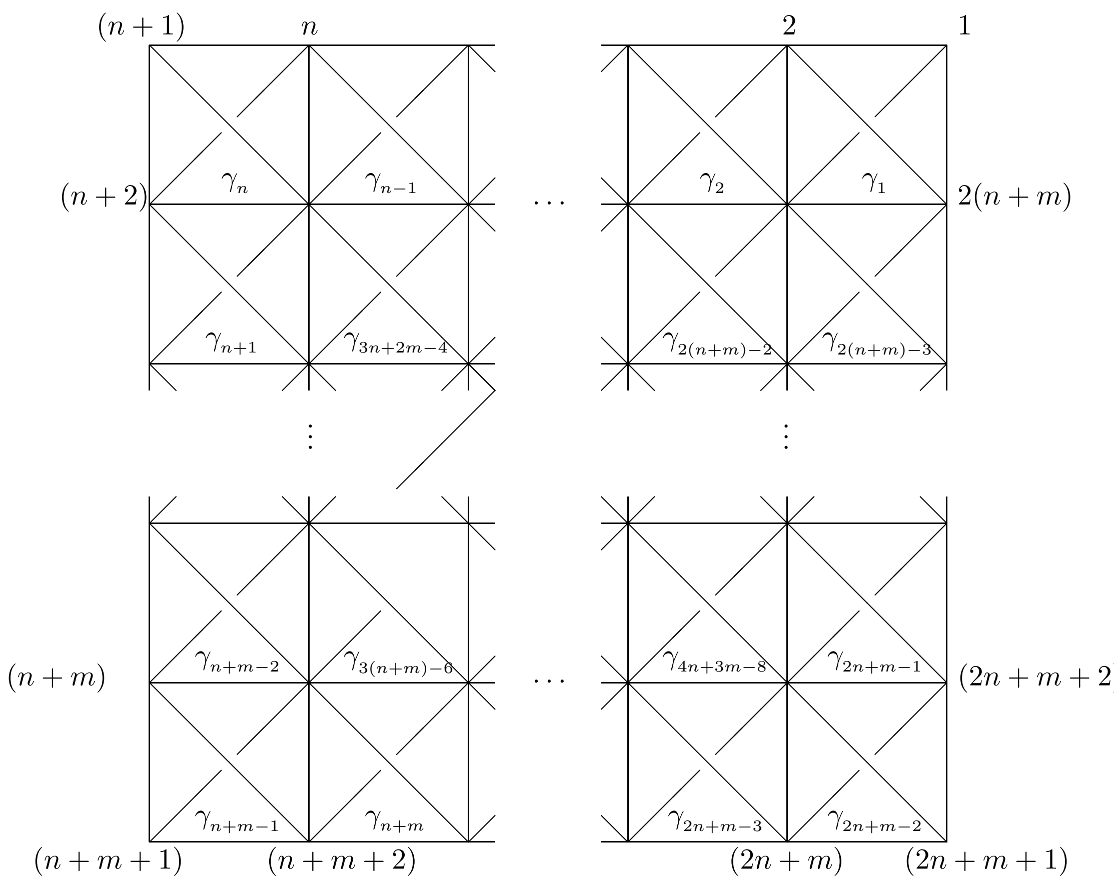

Figure 4: $(m\text{x}n)$-Tile Conductivity Network

negative ratio of conductivities at the left end of the tile row. So then, regardless of the number of columns (n), this network reduction requires that $c_1 = -(\frac{\gamma_n}{\gamma_{n-1}})$. Similarly, we know that the only contributing potential to the *boundary* current at node $(n+2)$ is in terms of the conductivity γ_n. So then γ_n is directly determinable by the response matrix Λ and thus c_1 can be written in terms of γ_{n-1} exclusively. In general, it should be noted that there are $(n-1)$ interior nodes along the bottom of this row network where we can apply Kirchhoff's Law to determine expressions for the $(n-1)$ unspecified *boundary* potentials c_i. Hence, aside from the *boundary* current at node $(n+1)$ which specifies conductivity γ_n exclusively, we have $(n+1)$ remaining equations from $\Lambda\phi = \psi$ by which to solve for $(n-1)$ conductivities. As each of the initially unspecified potentials in these equations have since been uniquely expressed in terms of the same $(n-1)$ conductivities, this linear system completely determines the entire top row of tile conductivities in the $(m\text{x}n)$-tile network.

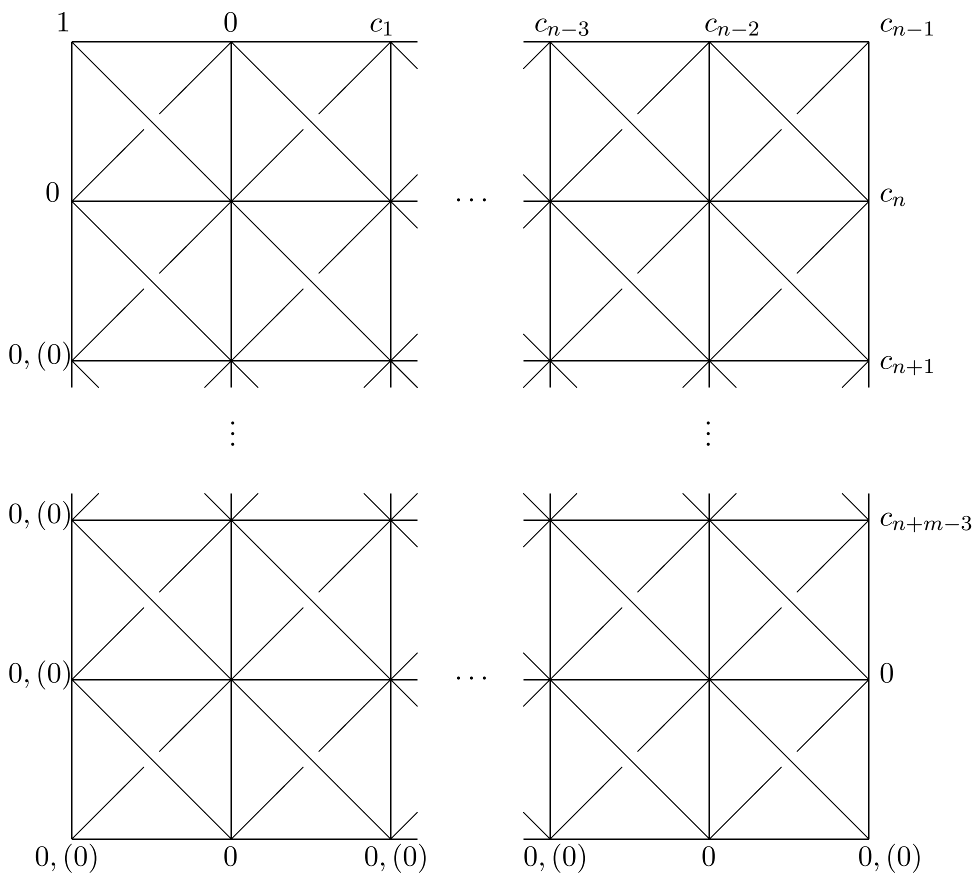

Figure 5: (mxn)-Tile Boundary Condition Configuration

So then, this recovery algorithm can be applied to each of the outer rows and columns of conductive tiles by rotation of *boundary* conditions, which facilitates the recovery of the outer-most rectangular ring of conductivities from the tile network. There remains, however, the problem of recovering the conductivites associated with the tiles on the interior of the rectangular network, which is addressed in the next section.

5 Recovering Interior Conductivities

5.1 First Interior Conductive Tile Ring

From the procedure described in § 4, let us now presume that the outer-ring of tile conductivities in our rectangular network has been recovered, which leaves us with an $(m-1)$x$(n-1)$ sub-network of undetermined conductivities. A proposed algorithm for determining the next inner-most rectangular ring of conductivities proceeds as follows. First let us impose a new set of

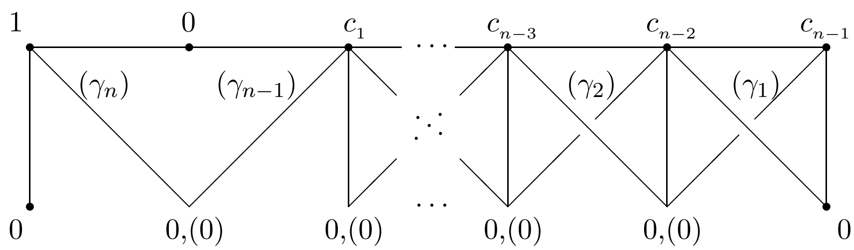

Figure 6: Reduced mxn-Tile Network

boundary conditions, as shown in Figure 7. Note from this diagram that we have imposed $(n + m + 3)$ *boundary* potentials with $(n + m - 3)$ overlapping currents, leaving $(n + m - 3)$ unknown *boundary* potentials – labeled $\{c_1, \ldots, c_{n+m-3}\}$. So then, by way of harmonic continuation, this network can be reduced to the one shown in Figure 8, where we have effectively removed all but the two top-most rows of conductive tiles.

Before we presume that a given conductivity recovery procedure will provide a unique solution for second (bottom-most) row of remaining tile conductivities, let us note a special characteristic of the reduced sub-network. In particular, stepping back to the original network prior to reduction we see through careful examination that this choice of *boundary* conditions allows for exactly one (unique) $(n+m-3)$-connection between the *boundary* nodes with unknown potentials $\{c_i\}$ and those with imposed currents. So then, as proven by Morrow [1] (p.49), we know that the misxed Dirichlet-Neumann problem for this network has a unique solution. Keeping in mind that we are in fact working with an optimization approximation, we state that this unique connection implies there exists a unique optimal approximation to the solution of the Dirichlet problem. As the diagram for arbitrarily large $(m$x$n)$ networks gets rather cluttered, and since the significant features of these networks arise for $m, n \geq 4$, the Figure 9 shows the pattern of these unique $(n + m - 3)$-connections for a (5x4) network.

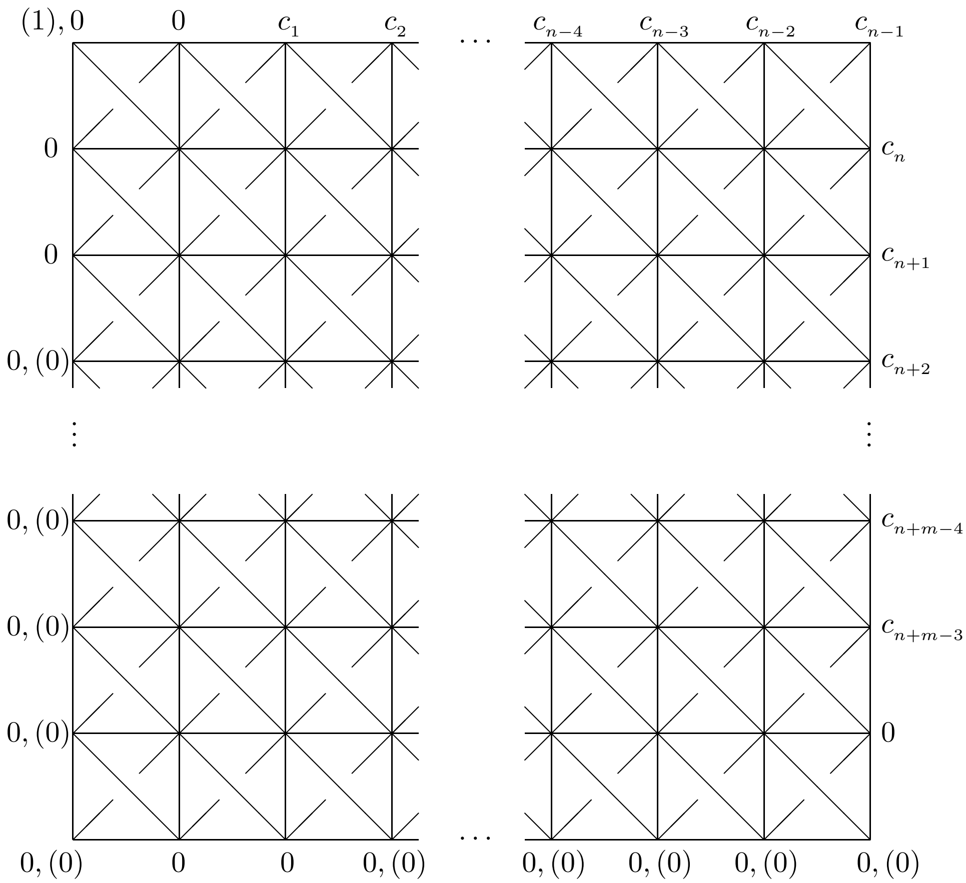

Figure 7: (mxn)-Tile Network with Alternative Boundary Conditions

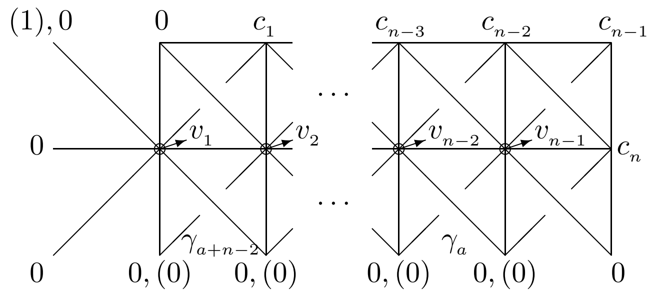

Figure 8: Reduced Alternative (mxn)-Tile Network

With uniqueness of potentials guaranteed, we may proceed with a tile conductivity recovery scheme. Let us recall, however, that in fact the conductivities for tiles around the outer ring are presumed known by the procedure outlined in § 4, leaving only γ_a through γ_{a+n-2} to be determined. Furthermore, the *interior* potentials v_1 through v_{n-1} are likewise unknown. So then, one proposed method begins by first computing the unknown *boundary* potentials from the system of equations corresponding to the specified *boundary* currents, which we know to be uniquely determined.

The algorithm proceeds by computing the unknown *interior* potential v_1 directly from the *boundary* current of 1 at the top-left node. From here, we begin an iterative process that will step across the two-row sub-network from left to right. Consider first the equation for boundary current ψ_n, entering the network at the node directly above that corresponding to *interior* potential v_1. Given the *boundary* current ψ_n and the previously determined *boundary* potential c_1, we can uniquely solve for the *interior* potential v_2. Subsequently, having determined v_2, we can form an equation generated by Kirchhoff's Law at the left-most bottom node with zero current that directly solves for the first unknown tile conductivity γ_{a+n-2}. The algorithm proceeds iteratively across the two-row sub-network employing the step just described. So then for some step i, we first form an equation for the *boundary* current ψ_{n+i-1} to solve for *interior* potential v_{i+1}, and subsequently write the equation generated by Kirchhoff's Law at sub-network *boundary* node $(n+3+i)$ to solve for unknown tile conductivity $\gamma_{a+n-1+i}$. Thus, by rotating this *boundary* condition configurtion for each each, and coupled with the outer-ring recovery algorithm decribed in § 4, we can completely solve for the two outer-most rings of tile conductivities.

5.2 Subsequent Interior Conductive Tile Rings

An algorithm to recover more deeply nested *interior* rings of tile conductivites is now derived in much the same respect as that just described for

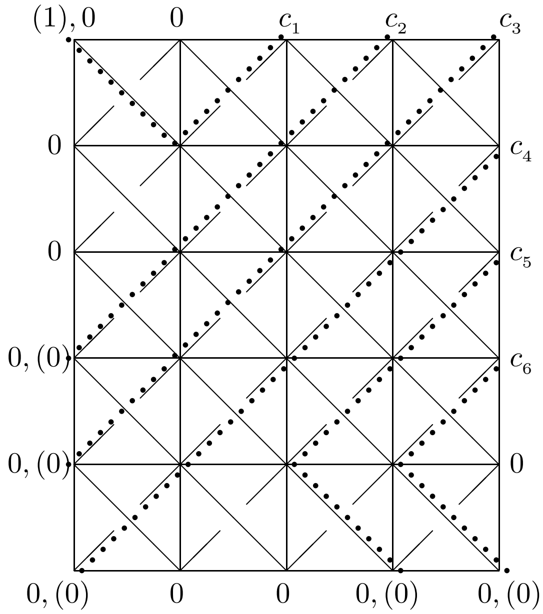

Figure 9: $(n + m - 3)$-Connection for a 5x4-Tile Network

the outer-most interior ring of conductive tiles. So then, recalling the *boundary* condition configuration denoted in Figure 7, consider the imposition of one fewer *boundary* conditions upon an $(m\text{x}n)$-tile network as shown in Figure 10. By application of Kirchhoff's Law, the underspecified network in Figure 10 can be reduced to that shown in Figure 11.

From the reduced sub-network shown in Figure 11, it should be recognizable that in fact we have only n remaining imposed *boundary* current, though there are in fact $(n + 1)$ unknown *boundary* potentials. Furthermore, since we imposed one fewer *boundary* condition than the number of *boundary* nodes in the network, let us impose one last current condition at the *boundary*. So then, we end up with the sub-network shown in Figure 12, where the unique $(n + 1)$-connection between imposed *boundary* currents and unknown *boundary* potentials is denoted by dotted lines.

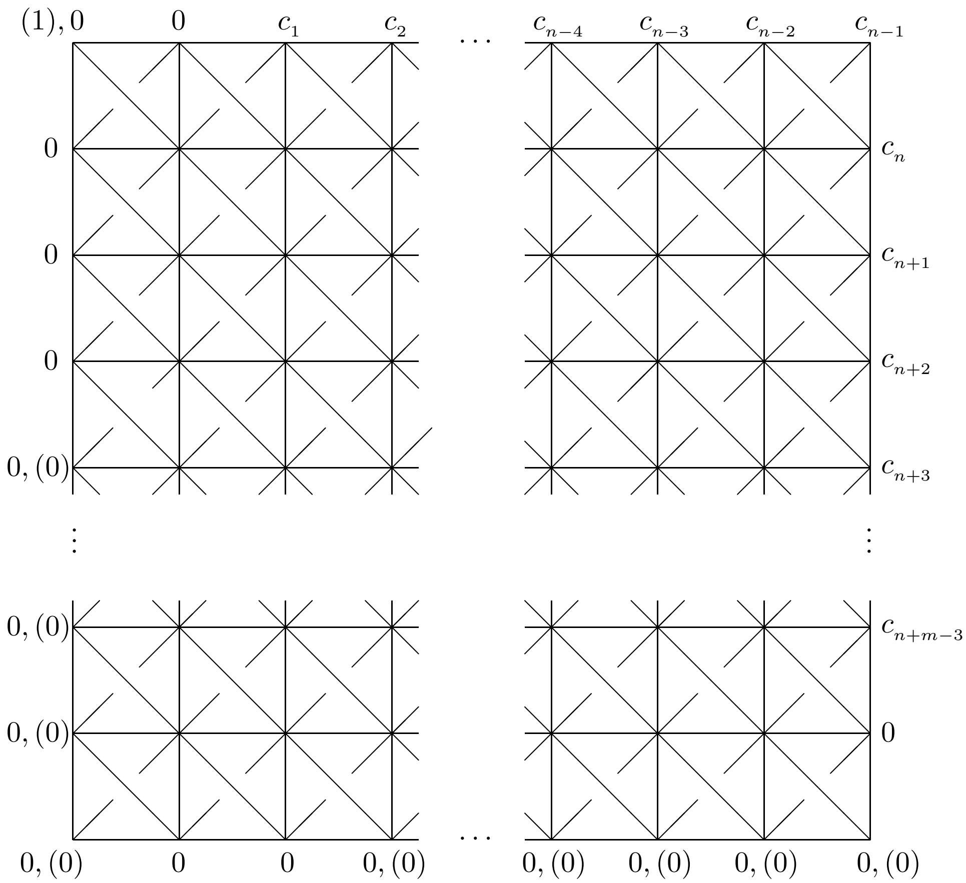

Figure 10: (mxn)-Tile Network with Alternative Boundary Conditions

At this point, the algorithm for recovery of the *interior* tile conductivities proceeds similarly to that described in § 5.1. Specifically, with respect to the labeling scheme in Figure 11, we first solve for the unknown *boundary* potentials from the system of equations generated by the imposed *boundary* currents. Next, solve directly for *interior* potential v_1 from *boundary* current ψ_{n+1}, and similarly for potential v_2 from *boundary* current ψ_{n+4}. Then begin the iterative step by computing *interior* potential v_3 from the equation generated by *boundary* current ψ_n, and subsequently solve for the first unknown inner tile conductivity from the equation for Kirchhoff's Law written at the sub-network *boundary* node $(n+5)$. Hence, for some iterated step i, we first compute the *interior* potential v_{2i+1} from the equation for *boundary* current ψ_{n+1-i}, and then solve for *interior* potential v_{2i+2} from the equation generated by Kirchhoff's Law at the node corresponding to potential v_{2i-1}. We then solve for the ith unknown inner tile conductivity from the equation generated by Kirchhoff's Law at the sub-network *boundary* node $(n+4+i)$.

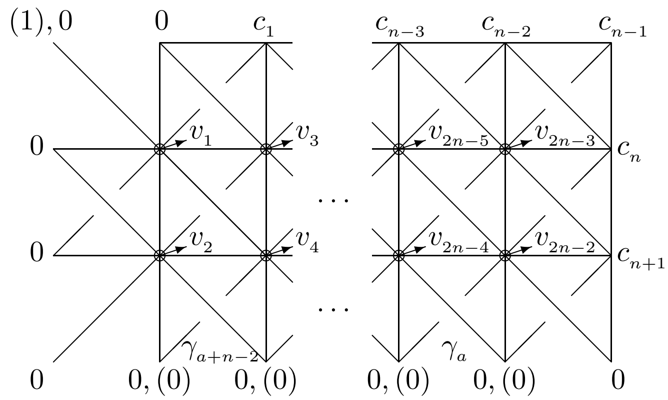

Figure 11: Reduced Alternative (mxn)-Tile Network

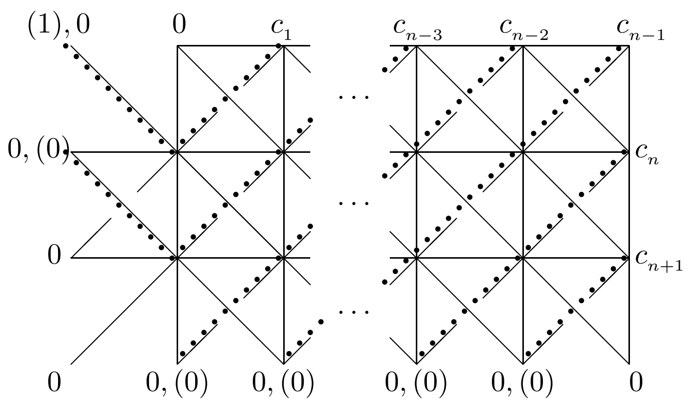

Figure 12: Reduced Alternative (mxn)-Tile Network with (n+1)-Connection

Hence, after $(n-2)$ iterations, and entire inner row of tile conductivities can be recovered by the *boundary* condition configuration describe in this section. Specifically, however, we needn't compute the first or last inner tile conductivities in this scheme, as they may be presumed known by the recovery procedure described in § 5.1.

5.3 Generalized Interior Recovery

In the previous two sections, algorithms were discussed for the direct recovery of *interior* rows of tile conductivities. By generalizing these procedural arguments, we can verify procedures for the entire recovery of an abitrary sized (mxn) network of equally sized conductive tiles. First, the outer ring of tile conductivities can be recovered by the algorithm described in § 4. The general algorithm then proceeds by iteratively recovering subsequent next-outer-most tile rings by the approach explicitly denoted in § 5.1 and §

5.2. The verification of this argument lies in the fact that this approach is legitimate for *interior* rows beyond two or three deep. To see this, note that the effective difference in boundary conditions between the configurations for recovering the first inner row and the next inner row was isolated to the altering of a single imposed *boundary* current. Essentially, as seen by comparing Figures 7 and 10 (together with the corresponding reduced networks), the adjustment necessary to recover the *next* inner row of tile conductivities is to move the position of nodes along the left side of the network without imposed *boundary* currents down by one. This then has the effect of leaving one more row of conductive tiles in the reduced sub-network. And given the similar arrangement of paths in the sub-network, this generalization allows for the recovery of the kth next inner row of tile conductivities. Hence, by repeated application of these iteratively altered *boundary* condition configurations, and by rotating like configurations to recover inner rows from all four sides within each iteration, an entire (mxn)-tile network is recoverable. This states the cumulative results of this paper.

6 Minimization of Energy in Three Dimensions

Consider the quadratic form of a power function in potential u discretized over a cubed region as

$$Q(u,u) = \sum_{k=1}^{M} \iiint_C \gamma_k |\nabla u_k|^2 \, \mathrm{d}V$$

Now, let us discretize the potential through a cube k by the piecewise trilinear (PT) function u_k, as this is uniquely determined by the eight values at the corners of cube k. For unit side-length cubes, and for a cubed network with respect to the normally oriented three-space origin, we then have

$$T_{0,0,0} = \begin{cases} (1-|x|)\,(1-|y|)\,(|z|-1) & |x|,|y|,|z| \le 1 \\ 0 & \text{otherwise} \end{cases}$$

$$T_{j,k,l} = T_{0,0,0}\,(j-x, k-y, l-z)$$

The PT potential function for a given cube k can then be written as a linear combination of contributing nodal trilinear potential functions, where the scalar coefficients α_{ik} in the following represent the potentials at the eight corners and T_{ik}'s represent the PT functions defined about the eight corners of cube k.

$$U_k = \sum_{i=1}^{8} \alpha_{ik} T_{ik}$$

This then gives us the final form of our power function Q as follows.

$$Q(u,u) \quad = \quad \sum_{k=1}^{M}\sum_{i,j=1}^{8} \gamma_k \alpha_{ik}\alpha_{jk} \iiint_C \left\langle \nabla T_{ik}, \nabla T_{jk} \right\rangle \mathrm{d}V \quad = \quad u^T K u$$

Noting that the symmetric quadratic form allows us to write the power function as $u^T Ku$, this suggests that we might be able to generate an analogous electrical network for this three-dimensional region with respect to the matrix K. Furthermore, by extracting K from the above inner-product form, we can generate the matrix elements $\kappa_{i,j}$ as

$$\kappa_{i,j} \quad = \quad \sum_k \gamma_k \iiint_C \left\langle \nabla T_{ik}, \nabla T_{jk} \right\rangle \mathrm{d}V$$

So then, let us test K for the necessary properties of Kirchhoff matrices. First, we know by construction that K is symmetric. Furthermore, since K is square it can be triangularized such that when u is a constant vector

$$K = Z^T Z \quad \Rightarrow \quad u^T Ku = u^T Z^T Zu = 0 \quad \Rightarrow \quad |Zu|^2 = 0$$

$$\Rightarrow \quad |Zu| = 0 \quad \Rightarrow \quad Z^T Zu = 0 \quad \Rightarrow \quad Ku = 0$$

which justifies that the row and column sums of K are indeed zero. So then, the last characteristic of Kirchhoff matrices to verify is that the off-diagonal elements are non-positive. This requires that we examine four possible cases of local support overlap for any two PT functions defined about given nodal points in space, which correspond to relationships amongst the coordinates about which the PTs are defined. Consider then a PT function T_i defined about the point (1,1,1) and another PT function T_j defined about the point (2,2,2). It should be readily verified that these two PT functions have overlapping support in exactly one cube, that defined by $x, y, z \in [1, 2]$. The PT functions T_i and T_j over this cube, and the entry κ_{ij} are then given by

$$T_i = (2-x)\,(2-y)\,(z-2) \qquad\qquad T_j = (x-1)\,(y-1)\,(1-z)$$

$$\kappa_{ij} = \gamma_k \int_1^2\!\!\int_1^2\!\!\int_1^2 \left\langle \nabla T_i, \nabla T_j \right\rangle \mathrm{d}x\,\mathrm{d}y\,\mathrm{d}z = -\left(\frac{\gamma_k}{12}\right)$$

which justifies the non-positive nature of off-diagonal entries in K corresponding to nodes that are a unit distance away from each other in all three dimensional directions. Next, consider the two PT functions defined about nodes that are a unit distance away from each other in any two dimensional directions. This entry in K connecting these nodes can be examined by the two PT functions T_i about (1,1,1) and T_j about (1,2,2), which overlap in the two-cube region defined by $x \in [0, 2]$ and $y, z \in [1, 2]$. The PT functions over half of this region and the entry κ_{ij} are then given by

$$T_i = (2-x)\,(2-y)\,(z-2) \qquad\qquad T_j = (2-x)\,(y-1)\,(1-z)$$

$$\kappa_{ij} = \gamma_{k1}\int_1^2\!\!\int_1^2\!\!\int_0^1 \left\langle \nabla T_i, \nabla T_j \right\rangle \mathrm{d}x\,\mathrm{d}y\,\mathrm{d}z = -\left(\frac{\gamma_{k1}}{12}\right)$$

Then noting that the PT functions are symmetric about the planar bisection of this two-cube region, and letting γ_{k1} and γ_{k2} represent the separate cube conductivities for these two cubes, this entire entry from K is given as

$$\kappa_{ij} = -\left(\frac{\gamma_{k1}+\gamma_{k2}}{12}\right)$$

and is thus shown to be non-positive. The next case involves nodes with one coordinate a unit distance away from each other, as with T_i defined about (1,1,1) and T_j defined about (1,1,2). The region of overlapping support is now defined by $x, y \in [0,2]$ and $z \in [1,2]$, or a slice of four cubes. To demonstrate an anomally about this configuration of neighboring nodes, let us first examine the component of this entry in K corresponding to the cube $x, y \in [0,1]$ and $z \in [1,2]$, which gives th following

$$T_i = (x)\,(y)\,(z-2) \qquad\qquad T_j = (x)\,(y)\,(1-z)$$

$$\kappa_{ij} = \gamma_{k1}\int_1^2\!\!\int_0^1\!\!\int_0^1 \left\langle \nabla T_i, \nabla T_j \right\rangle \mathrm{d}x\,\mathrm{d}y\,\mathrm{d}z = 0$$

Once again, by the symmetry of PT functions across the planar bisections of the four sub-cubes of overlapping support, each of the other three contributing integrals is shown to likewise be zero, and thus we get that κ_{ij} is non-positive.

The last possible configuration of neghboring nodes occurs when all three coordinates of the center points of PT functions are more than a unit distance apart from each other, which corresponds to two completely disjoint regions of PT support. Subsequently, the integral over the dotted gradients is zero. Hence, we have shown that all off-diagonal entries in the matrix K are non-positive. Together with the matrix symmetry and row/column sums equal to zero, we state here that in fact K is a Kirchhoff matrix [1], and therefore we can construct an electrical network analog for the discretized three-dimensional cubed region.

7 Cubed Network Construction

7.1 Current Paths in a Single Cube

From the derivation of our Kirchhoff matrix in § 6, the three-dimensional networks that follow should be treated as having current paths within each cube such that a path exists between every possible pair of diagonally opposing corners. This is, of course, presuming that the potentials associated with the eight corners are configured such to allow current flow. So then, we can think of each corner in a single cube as having four possible current paths, connecting it with those diagonally opposing corners along planar intersects and the single corner connected diagonally through the center point of the cube. For the interested reader, the plotting of such current paths within a single cube does present some interesting geometric considerations that will be exploited in later sections dealing with the recovery of cube conductivities.

7.2 Multi-Cube Network Orientation

Considering the (2x2x2)-cubed region in three space shown in Figure 13, let us define the vertex numbering scheme that we will use throughout the rest of this paper. Beginning with the top right-most node on the front-most face in Figure 13 [position (2,0,2)], number across from right to left, working down after completion of rows. This scheme numbers the nodes on the front-most face with 1 at the top-right-most node through 9 at the bottom-left-most node (0,0,0). After this, work toward the rear-most face in successive rings of *boundary* nodes, numbering as follows. Assign the next nodal number to the top-right-most node in the next *boundary* ring, and progress in a counter-clockwise order around one entire *boundary* ring. This scheme number the *boundary* nodes lying on the plane $y = 1$, starting with number 10 for the node located at potision (2,1,2) and continuing counter-clockwise until reaching number 17 for the node located at position (2,1,1). For any larger network, continue this *boundary* ring numbering scheme successively until reaching the rear-most face. Finally, for the rear-most face [in this case the plane $y = 2$], number in the same manner as with the front-most face. Specifically, starting with number 18 for the node at position (2,2,2) continue numbering along rows from right to left, and then working downward for successive rows until reaching number 26 for the node at position (0,2,0). The complexity of this problem in three dimensions should already be apparent.

For complexity purposes, we cannot display the Kirchhoff matrix even for this simple multi-cube network – a (27x27) matrix. To see many of the elemental forms except that corresponding to completely *interior* nodes, examine the Kirchhoff matrix for a twelve-node network consisting of two side-by-side unit cubes, and defined in the region $x \in [0, 2]$ and $y, z \in [0, 1]$. Considering conductivity γ_1 for the cube with $x \in [1, 2]$ and conductivity γ_2 for the cube with $x \in [0, 1]$, the Kirchhoff matrix is given by

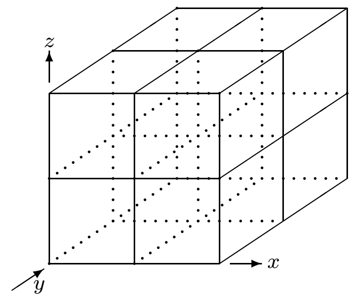

Figure 13: 2x2x2 Cubed Network

$$
K = \begin{pmatrix}
\frac{\gamma_1}{3} & 0 & 0 & 0 & -\frac{\gamma_1}{12} & 0 & 0 & -\frac{\gamma_1}{12} & 0 & 0 & -\frac{\gamma_1}{12} & -\frac{\gamma_1}{12} \\
0 & \frac{\left(\gamma_1+\gamma_2\right)}{3} & 0 & -\frac{\gamma_2}{12} & 0 & -\frac{\gamma_1}{12} & -\frac{\gamma_1}{12} & 0 & -\frac{\gamma_2}{12} & -\frac{\gamma_2}{12} & -\frac{\left(\gamma_1+\gamma_2\right)}{12} & -\frac{\gamma_1}{12} \\
0 & 0 & \frac{\gamma_2}{3} & 0 & -\frac{\gamma_2}{12} & 0 & 0 & -\frac{\gamma_2}{12} & 0 & -\frac{\gamma_2}{12} & -\frac{\gamma_2}{12} & 0 \\
0 & -\frac{\gamma_2}{12} & 0 & \frac{\gamma_2}{3} & 0 & 0 & 0 & -\frac{\gamma_2}{12} & -\frac{\gamma_2}{12} & 0 & -\frac{\gamma_2}{12} & 0 \\
-\frac{\gamma_1}{12} & 0 & -\frac{\gamma_2}{12} & 0 & \frac{\left(\gamma_1+\gamma_2\right)}{3} & 0 & -\frac{\gamma_1}{12} & 0-\frac{\left(\gamma_1+\gamma_2\right)}{12} & -\frac{\gamma_2}{12} & -\frac{\gamma_2}{12} & 0 & -\frac{\gamma_1}{12} \\
0 & -\frac{\gamma_1}{12} & 0 & 0 & 0 & \frac{\gamma_1}{3} & -\frac{\gamma_1}{12} & -\frac{\gamma_1}{12} & 0 & 0 & -\frac{\gamma_1}{12} & 0 \\
0 & -\frac{\gamma_1}{12} & 0 & 0 & -\frac{\gamma_1}{12} & -\frac{\gamma_1}{12} & \frac{\gamma_1}{3} & 0 & 0 & 0 & -\frac{\gamma_1}{12} & 0 \\
-\frac{\gamma_1}{12} & 0 & -\frac{\gamma_2}{12} & -\frac{\gamma_2}{12} & -\frac{\left(\gamma_1+\gamma_2\right)}{12} & -\frac{\gamma_1}{12} & 0 & \frac{\left(\gamma_1+\gamma_2\right)}{3} & 0 & -\frac{\gamma_2}{12} & 0 & -\frac{\gamma_1}{12} \\
0 & -\frac{\gamma_2}{12} & 0 & -\frac{\gamma_2}{12} & -\frac{\gamma_2}{12} & 0 & 0 & 0 & \frac{\gamma_2}{3} & 0 & -\frac{\gamma_2}{12} & 0 \\
0 & -\frac{\gamma_2}{12} & -\frac{\gamma_2}{12} & 0 & -\frac{\gamma_2}{12} & 0 & 0 & -\frac{\gamma_2}{12} & 0 & \frac{\gamma_2}{3} & 0 & 0 \\
-\frac{\gamma_1}{12} & -\frac{\left(\gamma_1+\gamma_2\right)}{12} & -\frac{\gamma_2}{12} & -\frac{\gamma_2}{12} & 0 & -\frac{\gamma_1}{12} & -\frac{\gamma_1}{12} & 0 & -\frac{\gamma_2}{12} & 0 & \frac{\left(\gamma_1+\gamma_2\right)}{3} & 0 \\
-\frac{\gamma_1}{12} & -\frac{\gamma_1}{12} & 0 & 0 & -\frac{\gamma_1}{12} & 0 & 0 & -\frac{\gamma_1}{12} & 0 & 0 & 0 & \frac{\gamma_1}{3}
\end{pmatrix}
$$

8 (mxnx1)-Cube Network Recovery

8.1 Outer Ring Recovery

In considering the explanation of recovery for an abitrary (mxnx1)-cube network, the significant features arise for $m, n \geq 4$. So then, take a (4x4x1)-cube network with numbering scheme as described in § 7, and consider the boundary condition configuration shown in Figure 14. For graphical clarity, the potentials specified at the nodes along the back and most of the bottom of this network are not shown, though all unspecified potentials in the figure below should be treated as having a value of zero. After application of an argument of harmonic continuation, the network is reduced to that shown in Figure 15.

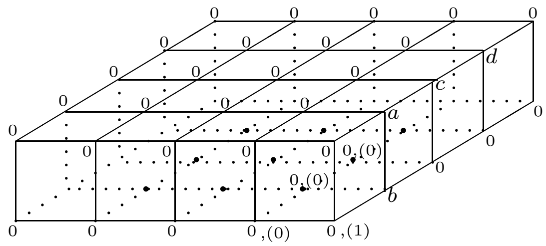

Figure 14: (4x4x1)-Cube Network with Boundary Conditions

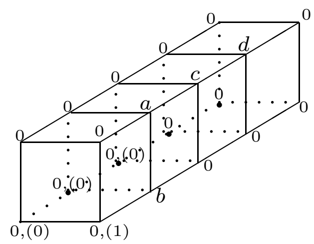

Figure 15: (4x4x1)-Cube Network with Boundary Conditions

As the above figure would become rather visually cluttered, the lines of unique connection have been excluded. It is then left to the reader to confirm that indeed there exists a unique connection between the imposed *boundary* currents and those *boundary* potentials left undetermined. So then, once again by the argument proven by Morrow [1], there exists a unique optimal approximation to our Dirichlet-Neumann problem, and thus we may solve directly and uniquely for the unknown *boundary* potentials $a, \ldots, d$ from the response matrix equations corresponding to the imposed *boundary* currents. With these computed, a recovery algorithm for the cube conductivities can proceed in a number of ways. For example, by starting at the top-left-front-most node and moving along the top-left-most row of nodes toward the rear (according to the spatial orientation in the previous figure) of the cubed network, we can solve successively for the cube conductivities from the equations for *boundary* current corresponding to these nodes. Hence, an outer row (or *bar*) and subsequently the entire outer ring of cube conductivites can be recovered in this manner.

8.2 Inner Cube Recovery

Consider now the (4x4x1)-cube network with modified *boundary* conditions shown in Figure 16. Note that the one unknown (and exclusively nonzero) *boundary* potential has been placed at the top node adjacent to all four unrecovered *interior* conductive cubes. This will subsequently generate current equations in each unknown conductivity separately.

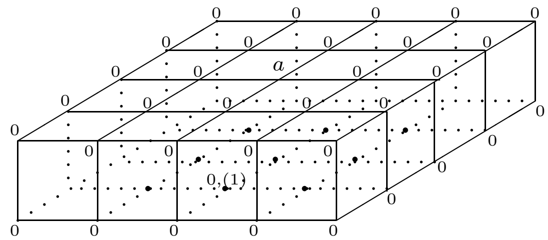

Figure 16: (4x4x1)-Cube Network with Boundary Conditions

The uniqueness of *boundary* potential should be easily confirmed, as there is only one *boundary* current-potential connection along possible intra-cube diagonals. Thus, the submatrix of the response matrix Λ corresponding to this pair is 1x1, nonzero, and subsequently the potential a is nonzero. So then, consider the sub-network shown in Figure 17, taken as the inner "sheet" of four conductive cubes adjacent to the node with potential a.

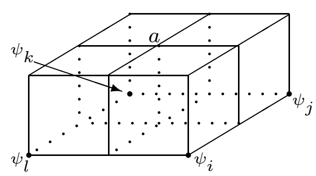

Figure 17: Inner 2x2x1-Cube Subnetwork Recovery Pattern

With this configuration of *boundary* potentials and currents, the four unknown cube conductivities can be recovered from the equations for the four *boundary* currents shown. For example, the conductivity of the cube with potential a and current ψ_k at opposite corners can be recovered as follows, letting the conductivity itself be termed γ_k.

$$\psi_k = (0 - a)\left(\frac{\gamma_k}{12}\right) \qquad \Rightarrow \qquad \gamma_k = -\left(\frac{12\psi_k}{a}\right)$$

Furthermore, by likewise solving for the three other inner "sheet" cube conductivities, we can recover the entire inner region. Hence, we can recover an entire (mxnx1)-cube network generated by our piecewise trilinear discretization of the continuous conductivity equation in three dimensions.

Appendix

Appendix 1 – Outer Ring Recovery in a (3x3)-Tile Network

Here we will demonstrate the recovery method for the outer ring of a (3x3)-tile network, as described generally in § 4. So then, consider the simplified network shown in Figure 18, as that reduced from a general (3x3)-tile network by imposition of the *boundary* condition configuration likewise described in § 4.

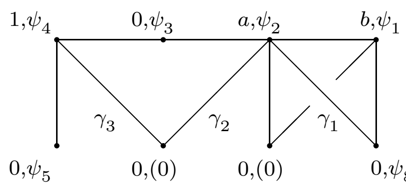

Figure 18: Outer Row Recovery in (3x3)-Tile Network

Next, note that since there are no *interior* nodes the Kirchhoff and Response matrices are in fact both given by

$$K = \Lambda = \begin{pmatrix} \frac{2\gamma_1}{3} & -\frac{\gamma_1}{6} & 0 & 0 & 0 & 0 & -\frac{\gamma_1}{3} & -\frac{\gamma_1}{6} \\ -\frac{\gamma_1}{6} & \frac{2(\gamma_1+\gamma_2)}{3} & -\frac{\gamma_2}{6} & 0 & 0 & -\frac{\gamma_2}{3} & -\frac{(\gamma_1+\gamma_2)}{6} & -\frac{\gamma_1}{3} \\ 0 & -\frac{\gamma_2}{6} & \frac{(\gamma_2+\gamma_3)}{3} & -\frac{\gamma_3}{6} & 0 & 0 & 0 & 0 \\ 0 & 0 & -\frac{\gamma_3}{6} & \frac{2\gamma_3}{3} & -\frac{\gamma_3}{6} & -\frac{\gamma_3}{3} & 0 & 0 \\ 0 & 0 & 0 & -\frac{\gamma_3}{6} & \frac{\gamma_3}{6} & 0 & 0 & 0 \\ 0 & -\frac{\gamma_2}{3} & 0 & -\frac{\gamma_3}{3} & 0 & \frac{(\gamma_2+\gamma_3)}{3} & 0 & 0 \\ -\frac{\gamma_1}{3} & -\frac{(\gamma_1+\gamma_2)}{6} & 0 & 0 & 0 & 0 & \frac{(3\gamma_1+\gamma_2)}{6} & 0 \\ -\frac{\gamma_1}{6} & -\frac{\gamma_1}{3} & 0 & 0 & 0 & 0 & 0 & \frac{\gamma_1}{2} \end{pmatrix}$$

At this point, let us presume that the respons matrix has been provided for a given set of conductive tiles. For example, applying unit conductivites to each of the tiles results in a numeric response matrix with values

$$\Lambda_1 = \begin{pmatrix} \frac{2}{3} & -\frac{1}{6} & 0 & 0 & 0 & 0 & -\frac{1}{3} & -\frac{1}{6} \\ -\frac{1}{6} & \frac{4}{3} & -\frac{1}{6} & 0 & 0 & -\frac{1}{3} & -\frac{1}{3} & -\frac{1}{3} \\ 0 & -\frac{1}{6} & \frac{2}{3} & -\frac{1}{6} & 0 & 0 & 0 & 0 \\ 0 & 0 & -\frac{1}{6} & \frac{2}{3} & -\frac{}{6} & -\frac{1}{3} & 0 & 0 \\ 0 & 0 & 0 & -\frac{1}{6} & \frac{1}{6} & 0 & 0 & 0 \\ 0 & -\frac{1}{3} & 0 & -\frac{1}{3} & 0 & \frac{2}{3} & 0 & 0 \\ -\frac{1}{3} & -\frac{1}{3} & 0 & 0 & 0 & 0 & \frac{2}{3} & 0 \\ -\frac{1}{6} & -\frac{1}{3} & 0 & 0 & 0 & 0 & 0 & \frac{1}{2} \end{pmatrix}$$

So then, we have that the *boundary* currents are given by $\Lambda\phi = \psi$, and subsequently we first solve for the unknown *boundary* potentials a and b from the zero currents along at the bottom nodes.

$$a = -\left(\frac{\Lambda_{6,4}}{\Lambda_{6,2}}\right) = -1 \qquad\qquad b = -a\left(\frac{\Lambda_{7,2}}{\Lambda_{7,1}}\right) = 1$$

From here, let us compute the numeric vector of *boundary* currents from the entirely determined vector of potentials.

$$\Lambda\phi = \begin{pmatrix} \frac{2}{3} & -\frac{1}{6} & 0 & 0 & 0 & 0 & -\frac{1}{3} & -\frac{1}{6} \\ -\frac{1}{6} & \frac{4}{3} & -\frac{1}{6} & 0 & 0 & -\frac{1}{3} & -\frac{1}{3} & -\frac{1}{3} \\ 0 & -\frac{1}{6} & \frac{2}{3} & -\frac{1}{6} & 0 & 0 & 0 & 0 \\ 0 & 0 & -\frac{1}{6} & \frac{2}{3} & -\frac{}{6} & -\frac{1}{3} & 0 & 0 \\ 0 & 0 & 0 & -\frac{1}{6} & \frac{1}{6} & 0 & 0 & 0 \\ 0 & -\frac{1}{3} & 0 & -\frac{1}{3} & 0 & \frac{2}{3} & 0 & 0 \\ -\frac{1}{3} & -\frac{1}{3} & 0 & 0 & 0 & 0 & \frac{2}{3} & 0 \\ -\frac{1}{6} & -\frac{1}{3} & 0 & 0 & 0 & 0 & 0 & \frac{1}{2} \end{pmatrix} \begin{bmatrix} 1 \\ -1 \\ 0 \\ 1 \\ 0 \\ 0 \\ 0 \\ 0 \end{bmatrix} = \begin{bmatrix} \frac{1}{2} \\ -\frac{5}{3} \\ 0 \\ \frac{2}{3} \\ -\frac{1}{6} \\ 0 \\ 0 \\ \frac{1}{6} \end{bmatrix}$$

At this point, we can begin to compute tile conductivities explicitly. First, note that the equation for *boundary* current at node 5 is given by

$$\psi_5 = -\Lambda_{5,4}(0-1) = \left(\frac{\gamma_3}{6}\right)(0-1) \quad \Rightarrow \quad -\left(\frac{1}{6}\right) = -\left(\frac{\gamma_3}{6}\right) \quad \Rightarrow \quad \gamma_3 = 1$$

which is concurrent with our numeric response matrix Λ_1. Next, we can recover γ_2 by considering the equation for *boundary* current at node 3.

$$\psi_3 = \Lambda_{3,4}(1-0) + \Lambda_{3,2}(0-a) = \left(\frac{-\gamma_3 + \gamma_2}{6}\right) = 0 \quad \Rightarrow \quad \gamma_2 = \gamma_3 \quad \Rightarrow \quad \gamma_2 = 1$$

which is likewise concurrent with our numeric response matrix Λ_1. Lastly, consider the equation for *boundary* current written at node 8.

$$\psi_8 = -\Lambda_{8,2}(0-a) + \Lambda_{8,1}(0-b) = \left(\frac{\gamma_1}{2}\right) = \frac{1}{2} \quad \Rightarrow \quad \gamma_1 = 1$$

which recovers the last unknown outer row tile conductivity from our numeric response matrix accurately. Thus, by applying this same approach to a rotated set of similar *boundary* for each of the remaining three sides of our (3x3)-tile network, we can recover the entire outer ring of tile conductivities from a given numeric response matrix.

Appendix 2 – Inner Ring Recovery in an (mx4)-Tile Network

Here we will demonstrate the recovery method for an inner ring of an (mx4)-tile network, as described generally in § 5. Consider the simplified network shown in Figure 19, as that reduced from a general (mx4)-tile network by imposition of the *boundary* condition configuration likewise described in § 5.

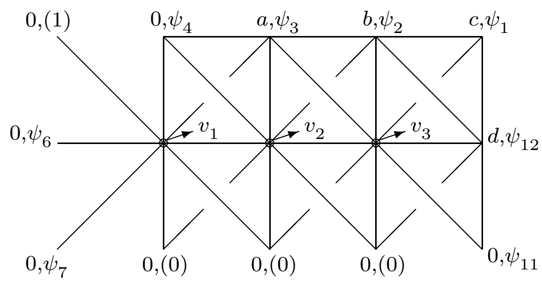

Figure 19: Inner Row Recovery in (mx4)-Tile Network

For complexity reasons, we have omitted the symbolic Kirchhoff and Response matrices, K and Λ. Suffice to say, however, that the elemental forms are completely analogous to those found in the Kirchhoff matrix corresponding to Figure 18. Consider, however, a presumed numeric response matrix (Λ_1) taken from a network with only unit conductivities, we have the following

$$\Lambda_1 = \begin{pmatrix}
\frac{929}{1488} & -\frac{319}{1488} & -\frac{3}{62} & -\frac{3}{496} & -\frac{1}{1488} & -\frac{1}{1488} & -\frac{1}{1488} & -\frac{3}{496} & -\frac{3}{62} & -\frac{71}{1488} & -\frac{21}{496} & -\frac{311}{1488} \\
-\frac{319}{1488} & \frac{1841}{1488} & -\frac{25}{93} & -\frac{27}{496} & -\frac{3}{496} & -\frac{3}{496} & -\frac{3}{496} & -\frac{27}{496} & -\frac{19}{186} & -\frac{143}{1488} & -\frac{71}{1488} & -\frac{189}{496} \\
-\frac{3}{62} & -\frac{25}{93} & \frac{110}{93} & -\frac{25}{93} & -\frac{3}{62} & -\frac{3}{62} & -\frac{3}{62} & -\frac{19}{186} & -\frac{14}{93} & -\frac{19}{186} & -\frac{3}{62} & -\frac{3}{62} \\
-\frac{3}{496} & -\frac{27}{496} & -\frac{25}{93} & \frac{1097}{1488} & -\frac{71}{1488} & -\frac{71}{1488} & -\frac{71}{1488} & -\frac{143}{1488} & -\frac{19}{186} & -\frac{27}{496} & -\frac{3}{496} & -\frac{3}{496} \\
-\frac{1}{1488} & -\frac{3}{496} & -\frac{3}{62} & -\frac{71}{1488} & \frac{433}{1488} & -\frac{21}{496} & -\frac{21}{496} & -\frac{71}{!488} & -\frac{3}{62} & -\frac{3}{496} & -\frac{1}{1488} & -\frac{1}{1488} \\
-\frac{1}{1488} & -\frac{3}{496} & -\frac{3}{62} & -\frac{71}{1488} & -\frac{21}{496} & \frac{433}{1488} & -\frac{21}{496} & -\frac{71}{1488} & -\frac{3}{62} & -\frac{3}{496} & -\frac{1}{1488} & -\frac{1}{1488} \\
-\frac{1}{1488} & -\frac{3}{496} & -\frac{3}{62} & -\frac{71}{1488} & -\frac{21}{496} & -\frac{21}{496} & \frac{433}{1488} & -\frac{71}{1488} & -\frac{3}{62} & -\frac{3}{496} & -\frac{1}{1488} & -\frac{1}{1488} \\
-\frac{3}{496} & -\frac{27}{496} & -\frac{19}{186} & -\frac{143}{1488} & -\frac{71}{1488} & -\frac{71}{1488} & -\frac{71}{1488} & \frac{283}{496} & -\frac{19}{186} & -\frac{27}{496} & -\frac{3}{496} & -\frac{3}{496} \\
-\frac{3}{62} & -\frac{19}{186} & -\frac{14}{93} & -\frac{19}{186} & -\frac{3}{62} & -\frac{3}{62} & -\frac{3}{62} & -\frac{19}{186} & \frac{79}{93} & -\frac{19}{186} & -\frac{3}{62} & -\frac{3}{62} \\
-\frac{71}{1488} & -\frac{143}{1488} & -\frac{19}{186} & -\frac{27}{496} & -\frac{3}{496} & -\frac{3}{496} & -\frac{3}{496} & -\frac{27}{496} & -\frac{19}{186} & \frac{1345}{1488} & -\frac{71}{1488} & -\frac{189}{496} \\
-\frac{21}{496} & -\frac{71}{1488} & -\frac{3}{62} & -\frac{3}{496} & -\frac{1}{1488} & -\frac{1}{1488} & -\frac{1}{1488} & -\frac{3}{496} & -\frac{3}{62} & -\frac{71}{1488} & \frac{227}{496} & -\frac{311}{1488} \\
-\frac{311}{1488} & -\frac{189}{486} & -\frac{3}{62} & -\frac{3}{496} & -\frac{1}{1488} & -\frac{1}{1488} & -\frac{1}{1488} & -\frac{3}{496} & -\frac{3}{62} & -\frac{189}{496} & -\frac{311}{1488} & \frac{1921}{1488}
\end{pmatrix}$$

For the above response matrix, based on presumed tile conductivities, the first step in our recover algorithm is once again to solve for the uniquely determinable *boundary* potentials labeled $a, \ldots, d$. This involves solving the system of equations given by

$$\Lambda\left(\{12,1,2,3\};\{5,8,9,10\}\right)\phi\left(\{12,1,2,3\}\right) \quad = \quad \begin{bmatrix} 0 \\ 0 \\ 0 \\ 0 \end{bmatrix}$$

Which leads to *boundary* values of

$$\begin{bmatrix} a \\ b \\ c \\ d \end{bmatrix} = \begin{bmatrix} -27 \\ 54 \\ -27 \\ 3 \end{bmatrix} \qquad \text{and} \qquad \begin{bmatrix} \psi_1 \\ \psi_2 \\ \psi_3 \\ \psi_4 \\ \psi_5 \\ \psi_6 \\ \psi_7 \\ \psi_{11} \\ \psi_{12} \end{bmatrix} = \begin{bmatrix} -\left(\frac{53}{2}\right) \\ 81 \\ -45 \\ \frac{9}{2} \\ 1 \\ 1 \\ 1 \\ \left(\frac{1}{2}\right) \\ -\left(\frac{35}{2}\right) \end{bmatrix}$$

Next, consider the equation for *boundary* current ψ_5, where we have

$$\psi_5 = 1 = (v_1 - 0)\,K_{5,15} = -v_1\left(\frac{\gamma_4}{3}\right) \qquad \Rightarrow \qquad v_1 = -\left(\frac{3}{\gamma_4}\right) = -3$$

Next, we begin the iterative step in this recovery algorithm by solving for the next unknown *interior* potential v_2 from the equation for *boundary* current at node 4. This gives us that $v_2 = f(\psi_4, a, v_1, \gamma_3) = 3$, and is thus uniquely determined from the known values of its parameters. Next, we can directly recover the first unknown conductivity by the equation for zero *boundary* current at node 8.

$$(v_1 - 0)\left(\frac{\gamma_5 + \gamma_6}{6}\right) = (0 - v_2)\,\frac{\gamma_6}{3} \qquad \Rightarrow \qquad \gamma_6 = -\left(\frac{v_1\gamma_5}{2v_2 + v_1}\right) = 1$$

So then, the first unknown conductivity has been recovered, and the iterative step can be continued by writing the equation for *boundary* current at node 3 to solve for $v_3 = f(\psi_3, a, b, v_1, v_2, \gamma_2, \gamma_3) = 0$. This then uniquely determines the unknown *interior* potential v_3, and lets us recover the second unknown tile conductivity from the equaton for zero current at node 9.

$$v_1\left(\frac{\gamma_6}{3}\right) + v_2\left(\frac{\gamma_6 + \gamma_7}{6}\right) + v_3\left(\frac{\gamma_7}{3}\right) = 0 \qquad \Rightarrow \qquad \gamma_7 = -\gamma_6\left(\frac{2v_1 + v_2}{2v_3 + v_2}\right) = 1$$

Hence, keeping in mind that the two outer ring tile conductivites γ_5 and γ_8 can be obtained by the recovery algorithm outlined in the previous section, we have recovered the entire inner row of unknown tile conducvitivies.

Appendix 3 – Mathematica Code used in Computations

In these Mathematica functions, the incoming arguments can be described as follows. For both functions, `lambda_` corresponds to a given numeric response matrix, `phi_` to a vector of boundary currents (first with unknown potentials, and later with determined numeric potentials), and `n_` to the number tiles in each row of the reduced sub-network. In the second function listed below, the last parameter `imposedGammas_` represents a set of rules for presumed known conductivities, such as those corresponding to the already recovered outer ring of conductive tiles.

```
            (*    Solve for Undetermined Boundary Potentials    *)

solveBoundary[lambda_, phi_, n_] := Block[{V = Table[vi, {i, 1, (n - 1)}],
            gammas = Table[γi, {i, 1, 2n}], psi = lambda.phi, temp},

    temp = Table[0, {i, 1, n}];
    temp[[1]] = Solve[psi[[n + 1]]-1 == 0, phi[[n - 1]]];

    phi = phi /.  temp[[1]][[1]];
    For[i = 2, i <= (n - 1),i++,
        temp[[i]] = Solve[psi[[n + 2 + i]] == 0, phi[[n - i]]];
        phi = phi /.  temp[[i]][[1]];
    ];
    temp[[n]] = Solve[psi[[2n + 2]] == 0, phi[[2n + 4]]];
    phi = phi /.  temp[[n]][[1]];

    Return[MatrixForm[Phi]]];
];

            (*    Recover Interior Tile Conductivities    *)

recoverTiles[lambda_, inPhi_, n_, imposedGammas_] := Block[{V = Table[vi, {i, 1, (n - 1)}],
            gammas = Table[γi, {i, 1, 2n}], phi = inPhi, psi = lambda.phi},

    V[[1]] = -(3 / gammas[[n]];
    V = V /.  Solve[(phi[[n]] - V[[1]])((gammas[[n]] + gammas[[n - 1]]) / 6)
            + (phi[[n]] - phi[[n - 1]])(gammas[[n - 1]] / 6) +
            (phi[[n]] - V[[2]])(gammas[[n - 1]] / 3) - psi[[n]] == 0,
            V[[2]]][[1]]//FullSimplify;
    gammas[[n + 2]] =- (V[[1]] * gammas[[n + 1]]) / (2*V[[2]] + V[[1]])//FullSimplify;

    V = V /.  Solve[(phi[[n - 1]])(gammas[[n - 1]] / 6)
            + (phi[[n - 1]] - V[[1]])(gammas[[n - 1]] / 3)
            + (phi[[n - 1]] - V[[2]])((gammas[[n - 1]] + gammas[[n - 2]]) / 6)
            + (phi[[n - 1]] - V[[3]])(gammas[[n - 2]] / 3) +
            (phi[[n - 1]]-phi[[n - 2]])(gammas[[n - 2]] / 6) - psi[[n - 1]] == 0,
            V[[3]]][[1]]//FullSimplify;
    gammas[[n + 3]] = -(gammas[[n + 2]])((2*V[[1]] + V[[2]]) / (2*V[[3]] + V[[2]]))//FullSimplify;

    Print[" v = ", MatrixForm[V], " = ", MatrixForm[V] /.  imposedGammas];
    Print[" γ6 = ", MatrixForm[gammas[[n + 2]]]];
    Print[" γ7 = ", MatrixForm[gammas[[n + 3]]]];
    Print[" γ = ", MatrixForm[gammas], " = ", MatrixForm[gammas /.  imposedGammas]]
];
```

References

[1] Morrow, James K. & Curtis, Edward B., *Inverse Problems for Electrical Networks*, Series on Applied Mathematics, Vol. 13, World Scientific, 2000.

[2] Duchamp, Thomas E., Discussions on piecewise bilinear functions as finite elements and optimization of elastic energy. University of Washington, Department of Mathematics, 2002.